Surface Science 144 (1984) 311–320
North-Holland, Amsterdam

RECONSTRUCTION OF THE (110) SURFACES FOR III–V SEMICONDUCTORS; FIVE SYSTEMS INVOLVING In OR Sb

Roger CHANG and William A. GODDARD III

*Arthur Amos Noyes Laboratory of Chemical Physics *, California Institute of Technology, Pasadena, California 91125, USA*

Received 5 March 1984; accepted for publication 3 May 1984

We report reconstruction geometries for the (110) surfaces of InSb, InAs, InP, GaSb, and AlSb based on theoretical calculations on cluster models. The surface strains are in excellent accord with experiment and the trends in surface strains fit well with the Duke linear lattice constant correlation. Surface reconstruction energies are in the range of 1.1 to 1.3 eV. We also report the geometries and energies for charged surface states.

1. Introduction

The reconstructed geometries of semiconductor surfaces determine the surface electronic states which in turn determine the chemical and electronic properties of the surface (e.g., Fermi-level pinning, Schottky barrier, initial steps of oxidation). Of particular interest has been the (110) surface of III–V zincblende-type systems, for several of which rather complete experimental and theoretical studies have been reported [1–7].

In this paper we extend the cluster calculations for X–Y semiconductors of Goddard and co-workers [8–10] (X = B, Al, Ga and Y = N, P, As) to include all combinations involving In or Sb (X = Al, Ga, In and Y = P, As, Sb). The calculated reconstruction geometries are compared with some recent experiments and analyzed in terms of lattice constant and electronegativity trends.

2. Results and discussion

The calculated surface shears, Δ, are quoted in table 1 for all nine cases considered here and compared with experiment in table 2 [5,11–18]. Δ is the perpendicular (to the surface) relative displacement of the two surface atoms. In seven of these cases there are experimental results, and for four systems

* Contribution No. 6991.

0039-6028/84/$03.00

Table 1
Summary for the reconstruction of the various III–V semiconductors; R_{XY} is the unreconstructed bond length and Δ is the perpendicular (to surface) z component of reconstruction strain (ΔZ_X and ΔZ_Y are the components for atoms X and Y, respectively)

Species XY	Surface strain Δ (Å)	Bulk bond length R_{XY} (Å)	Strain components		Reconstruction angle ω (deg)	Population at X		Population at Y	
			ΔZ_X (Å)	ΔZ_Y (Å)		Net charge [a]	Hybridization [b]	Net charge [a]	Hybridization [b]
InSb	0.779	2.8054	−0.531	0.248	27.9	+0.174	0.498	−0.174	0.637
GaSb	0.733	2.6394	−0.501	0.232	27.6	+0.144	0.503	−0.144	0.635
AlSb	0.735	2.6567	−0.502	0.233	27.9	+0.171	0.523	−0.171	0.638
InAs	0.691	2.6234	−0.474	0.217	26.0	+0.230	0.499	−0.230	0.660
GaAs	0.648	2.4479	−0.443	0.205	25.8	+0.200	0.504	−0.200	0.659
AlAs	0.645	2.4518	−0.442	0.203	26.1	+0.261	0.519	−0.261	0.662
InP	0.666	2.5412	−0.461	0.205	25.3	+0.297	0.498	0.297	0.667
GaP	0.628	2.3601	−0.432	0.196	25.7	+0.274	0.503	−0.274	0.669
AlP	0.629	2.3604	−0.437	0.192	25.3	+0.364	0.512	−0.364	0.673

[a] Based on Mulliken populations of H_2X or YH_2 units.
[b] Ratio of p population to s + p population, ignoring the small amount of d character (1 to 3%).

(AlP, GaAs, GaP, and GaSb) the theory and experiment agree to within 0.01 Å. For InP the disagreement is 0.02 Å (3%), for GaSb it is 0.04 Å (5%), and for InAs it is 0.09 Å (11%). As suggested by Duke [7], we compare the calculated and experimental strains with bond lengths R_{XY} in fig.1, leading to an excellent linear correlation with

$$\Delta(\text{Å}) = 0.388\, R_{XY} - 0.300.$$

Indeed, the theoretical results fit the relation better than do the experiments! Averaging these results, we find that Al and Ga lead to the same strain, whereas In has a strain 0.04 Å larger. In addition, As has a strain 0.02 Å larger than P and Sb a strain 0.09 Å larger than As. These trends are in rough accord with the atomic sizes.

Duke and co-workers [17] recently reported a second alternative for the GaAs(110) surface reconstruction. There are two quite different geometries consistent with analysis of the experimental LEED data using X-ray-type R factors, Case I (ref. [5]) with a total strain of $\Delta = 0.65$ Å (Ga down by 0.45 Å, As up by 0.20 Å) and a new, quite different configuration, Case II (ref. [17]) with a total strain of $\Delta = 0.172$ Å with As moving up from the (110) surface by 0.117 Å and Ga moving down by 0.055 Å. It was found that analysis of total intensities was able to distinguish these two structures, with the result that Case II is clearly not correct. We studied extensively the energy surface for displacements consistent with Case II but found no energy minimum near the region of the displacements reported in ref. [17]. In addition, the total energy for Case II was found to be 0.7 eV higher than Case I. Thus we concur that the Case II interpretation of GaAs(110) reconstruction does not occur.

Table 2
Comparison of theoretical and experimental values for surface strain Δ (experimental values in parentheses); all quantities in Å

	Al	Ga	In
P	0.629 (0.63) [a]	0.628 (0.63) [b]	0.666 (0.69) [c]
As	0.645	0.648 (0.65) [d]	0.691 (0.78) [e]
Sb	0.735	0.733 (0.77) [f]	0.779 (0.78) [g]

[a] Ref. [16].
[b] Ref. [13].
[c] Refs. [17,18].
[d] Ref. [5].
[e] Ref. [15].
[f] Ref. [12].
[g] Ref. [11].

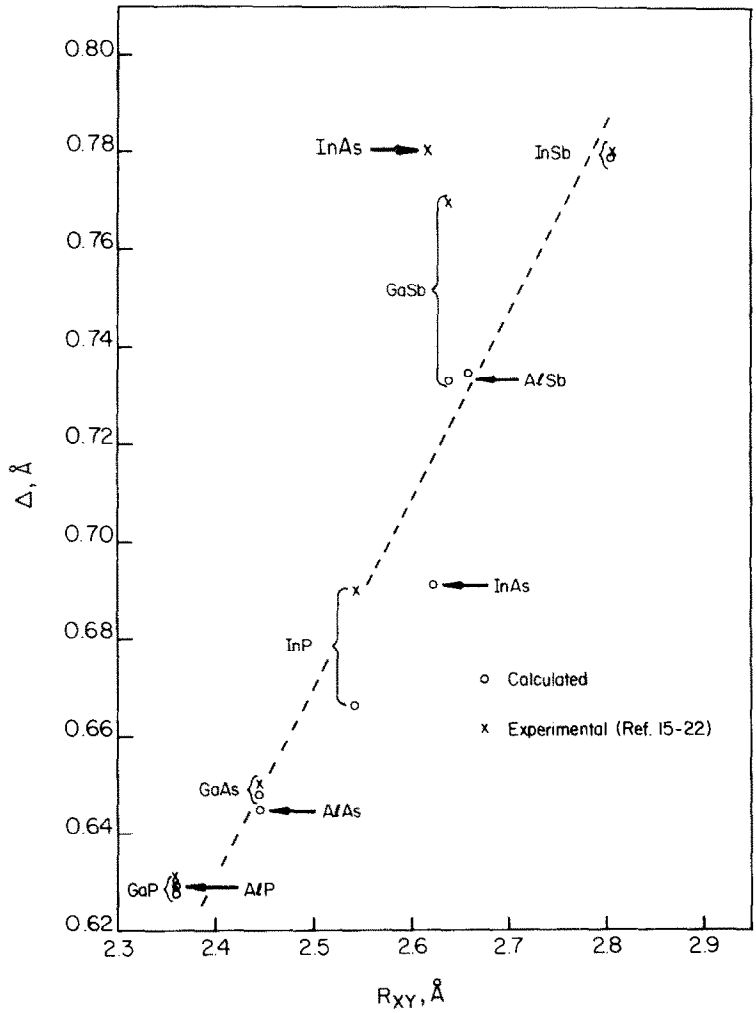

Fig. 1. Total surface strain Δ versus bond length R_{XY} for the nine XY semiconductors (X = Al, Ga, In; Y = P, As, Sb), comparison of theory (this work) and experiment (refs. [5,11–18]).

An alternative interpretation of the surface strain is in terms of the average bond angles of the surface atoms given in table 3, where we see that the average bond angle at the cation is always nearly planar (120°), while the bond angle at the anion is highly pyramidal (94–96°).

The reconstruction energies are shown in table 4. The range is 1.1 to 1.3 eV per pair of surface atoms. These energies are relevant for considering chemical processes at surfaces where the first step in bonding to a surface often leads to

Table 3
Average bond angles for the calculated structures; the angles calculated for XH_3 and YH_3 are shown in parentheses

	Al (120°)	Ga (120°)	In (120°)
P (94.8)	119.3	119.4	119.4
	96.1	95.8	96.1
As (94.3)	119.3	119.3	119.3
	95.9	95.8	95.9
Sb (93.6)	119.5	119.5	119.5
	94.5	94.9	94.9

unreconstruction to form tetrahedral coordination at the surface. To achieve this, the adsorbate must overcome the 1.1 to 1.3 eV reconstruction energy.

A very important role of reconstruction in the III–V's is the sweeping of surface donor and acceptor levels from the band gap so that for many cases the perfect surface does *not* give rise to pinning of the surface Fermi energy in the band gap. In order to gain some insight into this process, we calculated the energies for the neutral, positive ion, and negative ion in both the relaxed (reconstructed) and unrelaxed (tetrahedral) geometries. The results are shown in table 5. Because our complex does not have the whole array of X and Y atoms to represent the cleaved surface, the calculated levels are too deep for the donor and too shallow for the acceptor. However, the *shifts* in these levels with reconstruction should be reasonably well represented since the polarization effects would be similar for both geometries. Comparing tetrahedral with reconstructed geometries in table 5, we see that reconstruction pushes the donor levels 0.9 to 1.2 eV deeper while raising the acceptor levels by 0.9 to 1.3 eV. Both effects would tend to sweep surface levels out of the band gap. From empirical tight-binding calculations, Allen et al. [19] calculate that the minimum energy of the lowest occupied surface state, E_s, lies above the conduction band edge, E_c, by about 1.0 eV for InAs, about 0.5 eV for InSb and InP, and about 0.1 eV for GaAs. They also find that E_s lies somewhat below E_c for GaP. Allen [20] further predicted that there are no surface states within the band gap

Table 4
Reconstruction energies (in eV); differences between the energy for tetrahedral geometry versus optimum structure

	Al	Ga	In
P	1.14	1.20	1.12
As	1.12	1.17	1.11
Sb	1.20	1.25	1.18

a. Donor orbital (reconstructed)

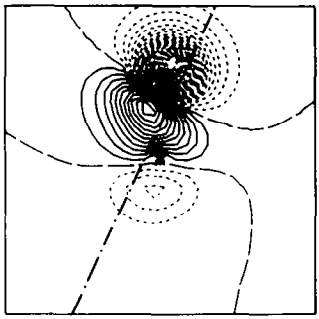

b. Donor orbital (tetrahedral)

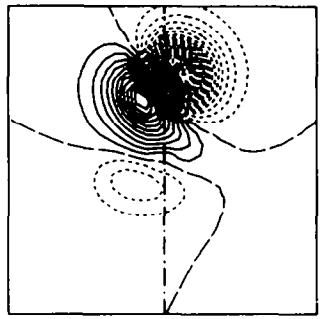

c. Acceptor orbital (reconstructed)

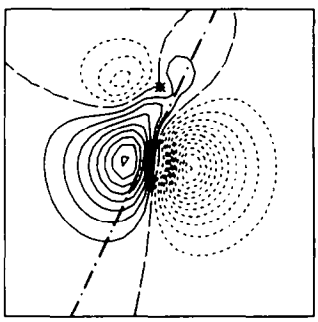

d. Acceptor orbital (tetrahedral)

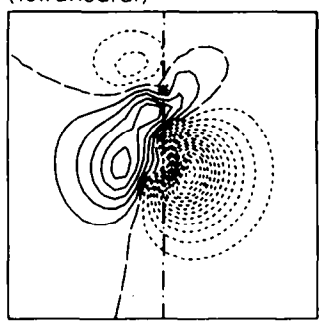

e. Lone pair orbital neutral state (reconstructed)

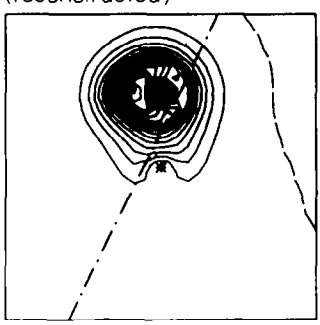

f. Bonding orbital neutral state (reconstructed)

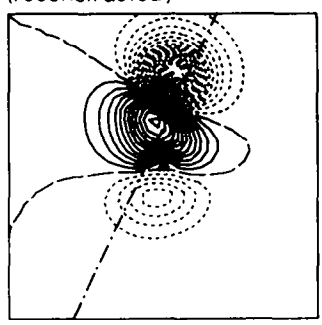

Table 5
Dependence of surface donor and acceptor levels upon reconstruction (in eV)

	Absolute energies				Energy shift	
	Reconstructed geometry [a]		Tetrahedral geometry [b]			
	Acceptor level [d]	Donor level [c]	Acceptor level [d]	Donor level [c]	Acceptor level	Donor level
AlP	+0.282	−8.287	−1.036	−7.073	+1.318	−1.214
GaAs	−0.206	−8.069	−1.067	−7.079	+0.861	−0.990
InSb	−0.042	−7.588	−1.342	−6.676	+1.300	−0.912

[a] Optimum geometry for neutral molecule.
[b] Unreconstructed tetrahedral geometry.
[c] Obtained as energy difference of SCF calculations between neutral molecule and negative ion (reconstructed and tetrahedral geometries).
[d] Same as footnote c between neutral molecule and positive ion.

of direct gap zincblende semiconductors such as GaAs, GaSb, InP, InAs, InSb, etc. For the indirect gap materials such as GaP and AlP, however, E_s is predicted to lie very near E_c. Since our calculations were restricted to small clusters, we could not differentiate between the direct gap and indirect gap materials.

In order to gain some insight into the nature of these relaxed states, we show the singly-occupied orbital of the donor state in figs. 2a and 2b for both the tetrahedral and the reconstructed geometries of the GaAs complex. Similar plots for the singly-occupied orbital for the acceptor state are shown in figs. 2c and 2d. The As lone pair orbital and the GaAs bonding orbital for the neutral complex are shown in figs. 2e and 2f for the reconstructed geometry.

The good agreement of our calculations with the experimental LEED values (table 2) as well as with other theoretical calculations (table 6) demonstrates that *the surface reconstruction is determined mainly by the local properties of the surface*, with the column III cation assuming a more or less planar geometry (bond angles close to 120°) and the column V anion a more or less pyramidal

Fig. 2. Selected orbitals for GaAs. (a, b) Donor orbitals from calculations on positive ion. (c, d) Acceptor orbitals from calculations on negative ion. (e, f) Orbitals from calculations on neutral molecule. The plot plane passes through the surface Ga (center) and surface As (upper center) atoms and is perpendicular to the original (110) surface. The surface plane for the unreconstructed surface is perpendicular to the plot plane and passes through both the surface Ga and As atoms in their unreconstructed positions. This surface trace is shown by the vertical dot-dash straight line (in b and d). For the reconstructed case, the trace of the original unreconstructed surface plane is shown by the slanted dot-dash lines in a, c, e, and f. Contour increments are 0.01 a.u., positive contours are solid lines, and negative contours are short dashed lines. Long dashed lines indicate zero amplitude.

Table 6
Comparison of theoretical results for the reconstruction strain (Δ in Å) with or without d-polarization functions

Compound XY	Hay EP [d]			SHC EP			Tight binding calculation [c]
	d on X, d on Y [a]	d on Y [a]	No d [a]	d on X, d on Y [b]	d on Y [a]	No d [b]	
InSb	–	0.779	0.783	–	–	–	0.818
GaSb	–	0.733	0.728	–	0.788	–	–
AlSb	–	0.735	0.750	–	–	–	–
InAs	–	0.691	0.672	–	–	–	–
GaAs	–	0.648	0.622	0.674	0.679	0.660	0.646
AlAs	–	0.645	0.634	0.673	–	0.662	–
InP	–	0.666	0.627	–	–	–	0.643
GaP	–	0.628	0.594	0.632	–	0.601	–
AlP	0.628 [d]	0.629 [d]	0.587 [d]	0.627 [d]	–	0.595 [d]	–

[a] Present work.
[b] Swarts and co-workers [10].
[c] Chadi [21].
[d] For Al and P, the SHC effective potentials were used. The small differences in Δ for AlP are due to the use of slightly different hydrogen basis sets in the calculations (5s/3s basis for the second, third, and fourth columns; 4s/2s basis for the fifth and seventh columns; see section 3).

geometry (bond angles 94 to 96°, close to the trihydride values). The calculated bond angles are summarized in table 3. Our calculations are limited to the top layer relaxation, while both the LEED data and Chadi's calculations [21] suggest further small changes in the subsurface layers. Since our results are in good agreement with the experimental results (as well as with the results of Chadi with respect to the top layer relaxation), we believe that the top layer relaxation is the dominant effect and that other geometry changes are of secondary importance. The good agreement discussed above suggests that the small cluster XYH_4 does indeed represent the (110) surface of the III–V semiconductors adequately for predicting the geometries and chemical properties.

3. Calculational details

The calculations used the same approach as reported by Swarts et al. [10]. Thus, the surface complex was modeled with a six-atom cluster

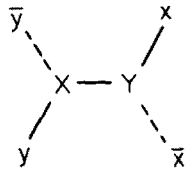

where X = Al, Ga, or In and Y = P, As, or Sb. In these calculations group III atoms at x and $\bar{x}$ were replaced by an H atom (using the bond distance for YH_3) pointing at the proper location (the image) for an X atom, and group V atoms at y and $\bar{y}$ were replaced by an H atom (using the bond distance of XH_3) pointing at the proper location (the image) for a Y atom. In the geometry variations, the images corresponding to subsurface atoms $\bar{x}$ and $\bar{y}$ were kept fixed, while X and x were moved together, and independently Y and y were moved together such that the bond distances $X\bar{y}$ and $Y\bar{x}$ were also kept fixed. Thus there were two degrees of freedom (one each for the perpendicular displacement of atoms X and Y) available in the structural optimization. This model has been shown to be adequate for calculating surface shear but cannot be used to assess the total relaxation of the surfaces layer with respect to subsurface layers.

In tables 2 and 3 we used the ab initio core effective potential of Wadt and Hay [22] for Ga, In, As, and Sb, and the SHC core effective potential of Rappé et al. [23] for Al and P. In table 6 we also carried out some calculations for Ga, As, and Sb using SHC core effective potentials. All calculations used the normal double zeta s, p basis sets, and the final structural optimizations used d basis functions on the group V atoms ($\alpha_P = 0.37$, $\alpha_{As} = 0.39$, $\alpha_{Sb} = 0.27$), where the exponents were optimized with HF calculations on YH_3.

The basis set used on the H's was the Huzinaga [24] 5s primitive basis contracted to 3s (no scaling). This differs slightly from the unscaled Huzinaga double zeta hydrogen 4s basis contracted to 2s used for some of the calculations described in table 2.

Table 6 compares results for various basis sets. Here we see that d functions are required on the anion but not on the cation. The theoretical (tight-binding) results of Chadi [21] are also listed in table 6 for comparison.

Acknowledgments

This research was supported in part by a contract (No. N00014-79-C-0797) from the Office of Naval Research. We thank Drs. Willard R. Wadt and P. Jeffrey Hay (Los Alamos National Laboratory) for use of the core effective potentials prior to publication.

References

[1] A.R. Lubinsky, C.B. Duke, B.W. Lee and P. Mark, Phys. Rev. Letters 36 (1976) 1058.
[2] S.Y. Tong, A.R. Lubinsky, B.J. Mrstik and M.A. Van Hove, Phys. Rev. B17 (1978) 3303.
[3] A. Kahn, E. So, P. Mark, C.B. Duke and R.J. Meyer, J. Vacuum Sci. Technol. 15 (1978) 1223.
[4] D.J. Miller and D. Haneman, J. Vacuum Sci. Technol. 15 (1978) 1267.

[5] R.J. Meyer, C.B. Duke, A. Paton, A. Kahn, E. So, J.L. Yeh and P. Mark, Phys Rev. B19 (1979) 5194.
[6] C.B. Duke, R.J. Meyer, A. Paton, J.L. Yeh, J.C. Tsang and A. Kahn, J. Vacuum Sci. Technol. 17 (1980) 501.
[7] C.B. Duke, J. Vacuum Sci. Technol. B1 (1983) 732.
[8] W.A. Goddard III, J.J. Barton, A. Redondo and T.C. McGill, J. Vacuum Sci. Technol. 15 (1978) 1274.
[9] J.J. Barton, W.A. Goddard III and T.C. McGill, J. Vacuum Sci. Technol. 16 (1979) 1178.
[10] C.A. Swarts, T.C. McGill and W.A. Goddard III, Surface Sci. 110 (1981) 400.
[11] R.J. Meyer, C.B. Duke, A. Paton, J.L. Yeh, J.C. Tsang, A. Kahn and P. Park, Phys. Rev. B21 (1980) 4740.
[12] C.B. Duke, A. Paton and A. Kahn, Phys. Rev. B27 (1983) 3436.
[13] C.B. Duke, A. Paton, W.K. Ford, A. Kahn and J. Carelli, Phys. Rev. B24 (1981) 562.
[14] B.W. Lee, R.K. Ni, M. Masud, X.R. Wang, D.C. Wang and M. Rowe, J. Vacuum Sci. Technol. 19 (1981) 294.
[15] C.B. Duke, A. Paton, A. Kahn and C.R. Bonapace, Phys. Rev. B27 (1983) 6189.
[16] C.B. Duke, A. Paton, A. Kahn and C.R. Bonapace, Phys. Rev. B28 (1983) 852.
[17] C.B. Duke, S.L. Richardson, A. Paton and A. Kahn, Surface Sci. 127 (1983) L135.
[18] R.J. Meyer, C.B. Duke, A. Paton, J.C. Tsang, J.L. yeh, A. Kahn and P. Park, Phys. Rev. B22 (1980) 6171.
[19] R.P. Beres, R.E. Allen and J.D. Dow, Phys. Rev. B26 (1982) 5702.
[20] R.E. Allen, Surface Sci. 110 (1981) L625.
[21] D.J. Chadi, Phys. Rev. B19 (1979) 2074.
[22] W.R. Wadt and P.J. Hay, to be published.
[23] A.K. Rappé, T.A. Smedley and W.A. Goddard III, J. Phys. Chem. 85 (1981) 1662.
[24] S. Huzinaga, J. Phys. Chem. 42 (1965) 1293.